Electronic Supplementary Material (ESI) for Sustainable Energy & Fuels.


# Supporting Information

# Photoelectrochemical Water Oxidation of $GaP_{1-x}Sb_x$ with a Direct Band Gap of 1.65 eV For Full Spectrum Solar Energy Harvesting

Mahdi Alqahtani[1,2], Sanjayan Sathasivam[3], Lipin Chen[4], Pamela Jurczak[1], Rozenn Piron[4], Christophe Levallois[4], Antoine Létoublon[4], Yoan Léger[4], Soline Boyer-Richard[4], Nicolas Bertru[4], Jean–Marc Jancu[4], Charles Cornet[4]*, and Jiang Wu[1]*, Ivan P. Parkin[3]*

[1]*Department of Electronic and Electrical Engineering, University College London, London WC1E 7JE, United Kingdom*

[2]*King Abdulaziz City for Science and Technology, Riyadh 12371, Saudi Arabia*

[3]*Department of Chemistry, University College London, London WC1H 0AJ, United Kingdom*

[4]*Univ Rennes, INSA Rennes, CNRS, Institut FOTON – UMR 6082, F-35000 Rennes, France*

**E-mail:charles.cornet@insa-rennes.fr , jiang.wu@ucl.ac.uk, and i.p.parkin@ucl.ac.uk.*

**X-ray photoelectron spectroscopy (XPS)**

Surface properties of as-grown $GaP_{0.67}Sb_{0.33}$ on Si substrate were inferred from X-ray photoelectron spectroscopy (XPS). The XPS survey scan (fig. S1 a) shows the expected Ga, P, Sb, O and C transitions on the surface. Fig S1b shows the Ga 2p transition with the Ga $2p_{3/2}$ peak centred at 1117.0 eV, which matches literature for Ga in the 3+ oxidation state and bound to species such as P or As.[1] The Ga 3d peak (Fig S1c) however shows a clear shoulder and thus can be deconvoluted with two sets of doublets therefore suggesting two different Ga environments. The primary Ga $3d_{5/2}$ peak centred at 19.1 eV corresponds to Ga 3+ bound to P whereas the secondary Ga $3d_{5/2}$ peak centred at 20.6 eV matches Ga bound to O in the native oxide $Ga_2O_3$.[2, 3] P 2p region shows two peaks that can be deconvoluted with the primary $2p_{3/2}$ peak at 128.8 eV and matching P in the -3 oxidation state and therefore corresponding to P bound to Ga in GaP (fig S1d).[2, 3] The secondary $2p_{3/2}$ peak at 133.3 eV matches P in the 5+ oxidation state and maybe attributed to native oxide species.[2, 3] Two Sb environments can be seen, a Sb $3d_{5/2}$ peak at 530.2 eV corresponding to Sb in the 3+ oxidation state.[4, 5] An additional Sb $3d_{5/2}$ peak at 527.3 eV is too low in energy to correspond to metallic Sb, which is often found at 528.0 eV, therefore we believe this peak at 527.3 eV corresponds to Sb in the -3 oxidation state and in the form of GaSb. Previous XPS studies of GaSb have focused only on the Sb 4d transition therefore comparison of this peak to literature values is not possible.[6, 7]

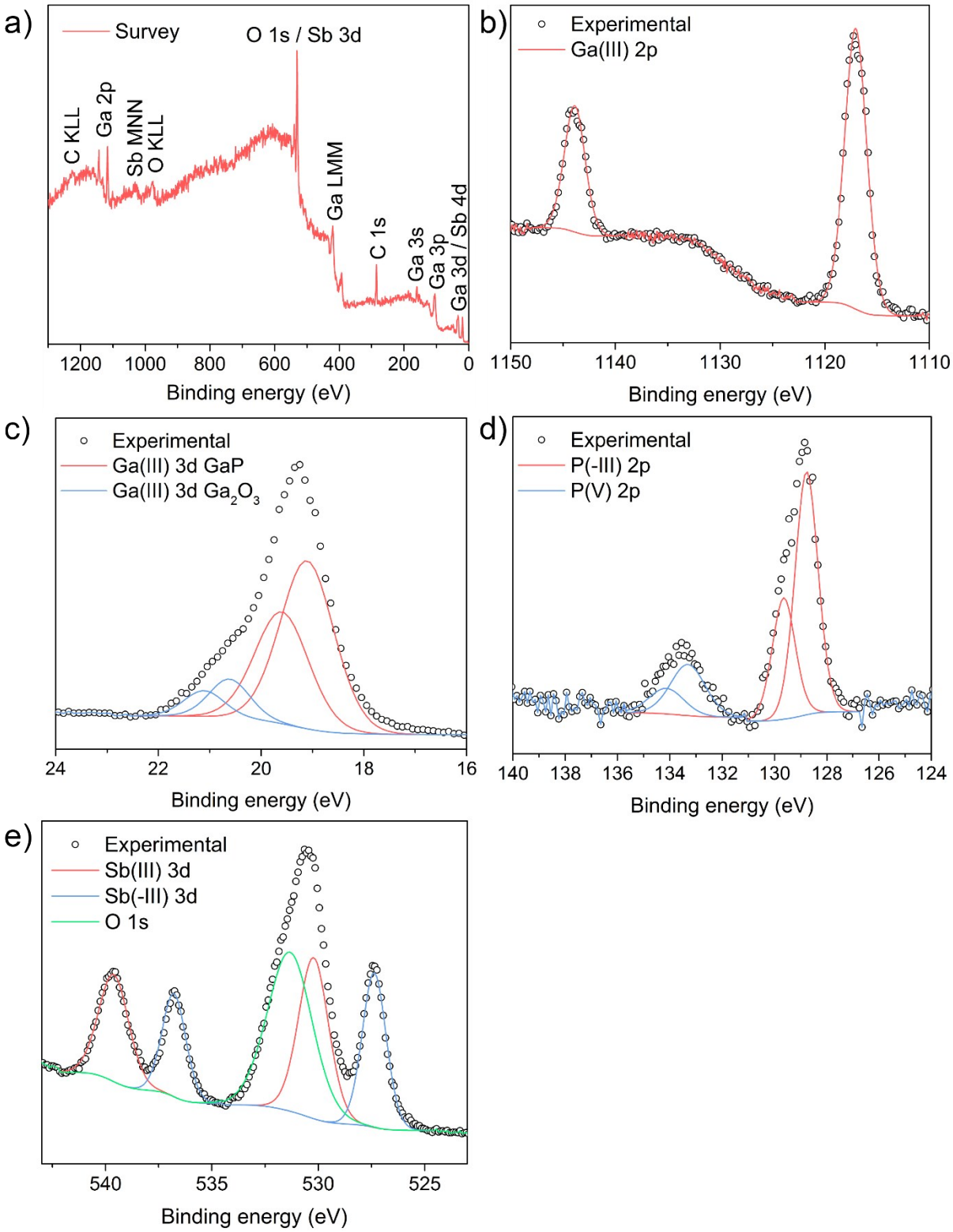


**Figure S1.** XPS results showing the (a) survey scan showing the expected Ga, P, Sb and O and C transitions and the high resolution (b) Ga 2p, (c) Ga 3d, (d) P 2p and (e) Sb 3d/O 1s transitions.

**X-Ray diffraction reciprocal space mappings (RSM)**

X-Ray diffraction reciprocal space mappings (RSM) around the (224) (Fig. S2 a)) and the (004) (Fig. S2 b)) Bragg peaks, have been used to assess the crystal structural properties.

A miscut of 6.1+-0.05° is first observed toward the [110] direction, from positions of Si Bragg peaks, in agreement with the substrate specifications. The Reciprocal space maps carried out on either (224) and (004) reflections show a full plastic relaxation of the $GaP_{0.67}Sb_{0.33}$ layer. The $GaP_{0.67}Sb_{0.33}$ lattice parameter has been extracted from RSM, confirming the full plastic relaxation rate and giving a mean lattice parameter of 0.5665±0.0005 nm. A Sb content of 0.33+-0.01 in $GaP_{0.67}Sb_{0.33}$ is then inferred from these values, following the Vegard's law[8]. The observed position of the $GaP_{0.67}Sb_{0.33}$ peaks overpasses the relaxation line (bold dashed line in both mappings). This actually corresponds to a supplementary tilt of the order of 0.4°. This is classically interpreted as the contribution of the miscut on plastic relaxation process. First, a $\Delta\alpha$ Nagai angle of 0.25° is calculated upon:

$$tan(\Delta\alpha) = \frac{(a_{op} - a_S)}{a_S} tan(\alpha) \quad \text{(eq. 1)}$$

where $\alpha$ is the miscut value. $a_{op}$ is the out of plane lattice parameter of the layer (here the measured value) and $a_S$ is the substrate lattice parameter[9]. A supplementary tilt of the order of 0.15° and a large broadening of the reflections are observed in agreement with a large density of 60°-degree misfit dislocations.

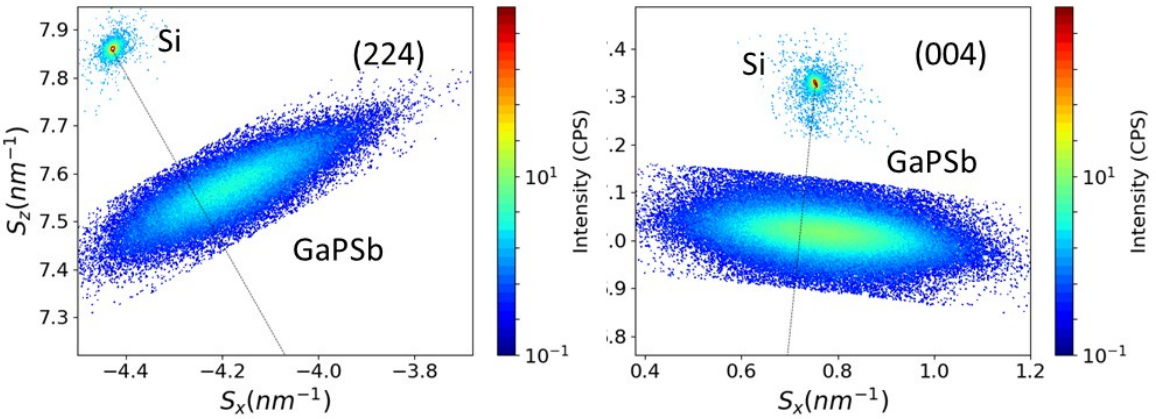


**Figure S2.** X-Ray diffraction reciprocal space mappings of the $GaP_{0.67}Sb_{0.33}$/Si photoanode around the (a) (224) and (b) the (004) Bragg positions. The black line represents the full relaxation line.

**Ellipsometry Measurement**:

The optical constants of the $GaP_{0.67}Sb_{0.33}$ alloy was measured by variable angle spectroscopic ellipsometry (VASE) at room temperature in the 0.85–5 eV photon energy region. The angles of incidence were set to 60˚ and 70˚. A Tauc-Lorentz model with 2 oscillators was used to fit the ellipsometry data and extract the absorption coefficient value. Fig. S3 a) shows the fitting result. The red and blue lines correspond to experimental spectra where $I_s$ and $I_c$ parameters are represented. $I_s$ and $I_c$ are related to the well-known ellipsometry variables ψ (amplitude component) and Δ (phase difference) through the following relations: $I_s = \sin(2\psi).\sin(\Delta)$, $I_c = \sin(2\psi).\cos(\Delta)$. The black lines correspond to the theoretical curves after adjusting the parameters of the Tauc-Lorentz model. From this model, the refractive index (n), extinction coefficient (k) and absorption spectrum of the sample were extracted, as shown in Fig.S3 b) and Fig.S3 c).

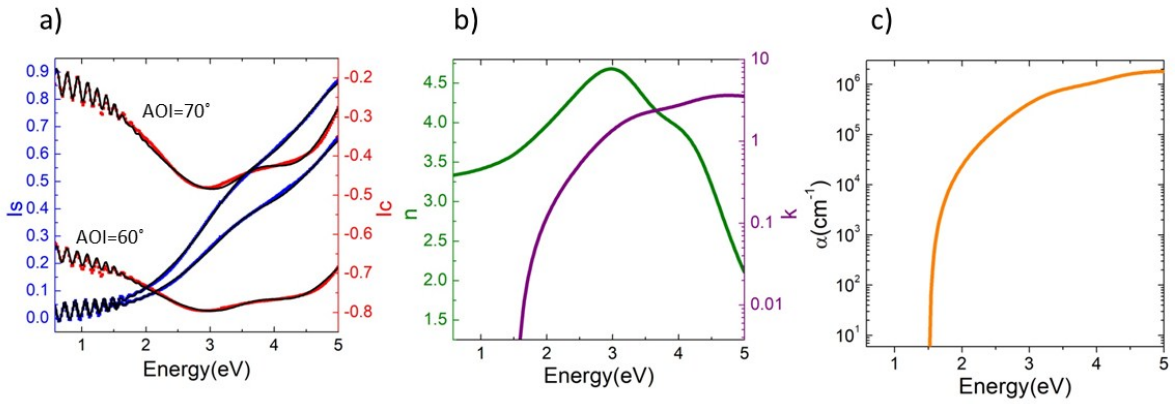


**Figure S3.** (a) Experimental ellipsometry spectra of $I_s$ and $I_c$ for two incidence angles (red and blue lines) and comparison with theoretical curves by using a 2-oscillators Tauc-Lorentz model (black lines). (b) n (optical index real part) and k (optical index imaginary part) optical constants extracted from the fitting of (a) and (c) optical absorption spectrum deduced from these measurements, showing a bandgap absorption edge at 1.65 eV.

**Photoelectrochemical measurements:**

XPS survey scan performed on the $TiO_2$ and Ni coated $GaP_{0.67}Sb_{0.33}$ is shown in Fig S4. It indicates the presence of only Ti, Ni, O and adventitious C on the surface of the film thus showing the successful formation of impurity free $TiO_2$ and Ni via ALD. Fig S5 shows the XPS of Ni 2p and confirms the presence of Ni and surface oxide NiO. A survey scan that was also performed shows that only Ni, O and C were found on the surface.

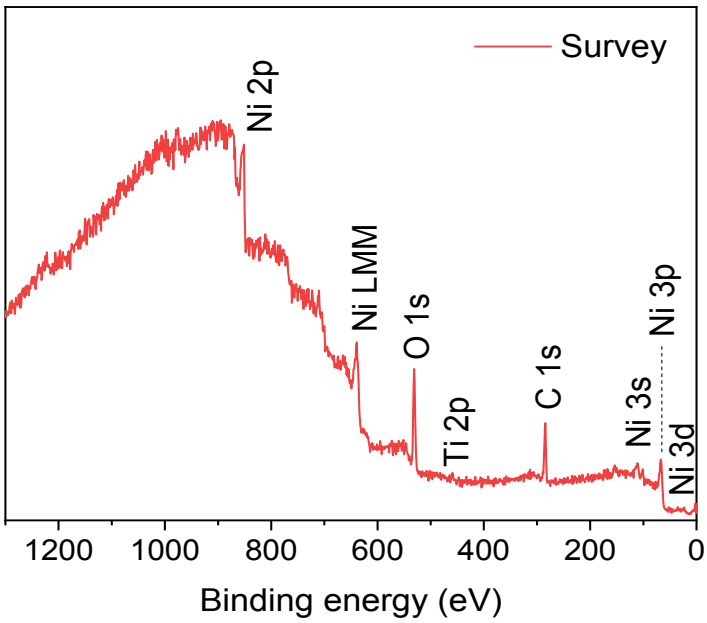


**Figure S4.** XPS results showing the survey scan for $GaP_{0.67}Sb_{0.33}$ coating with $TiO_2$ 20 nm and Ni 8 nm photoanode.

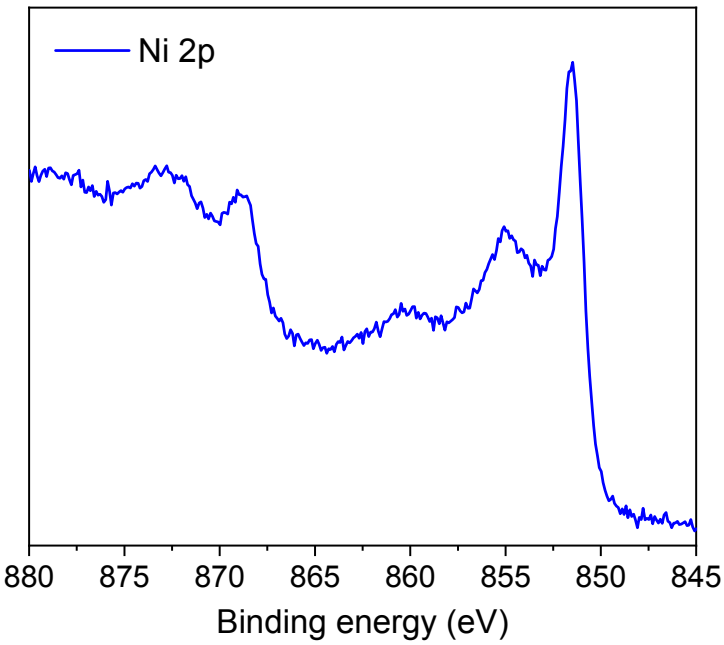


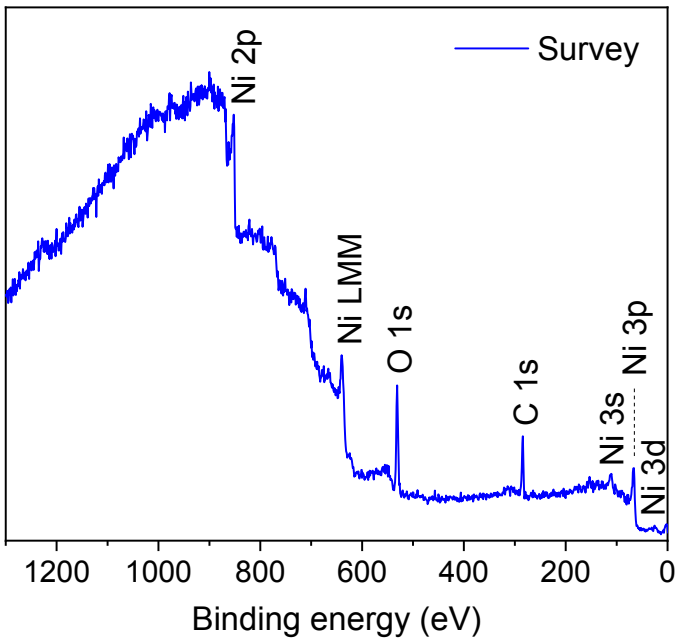


**Figure S5.** XPS results showing the surface (a) and (b) survey scan for $GaP_{0.67}Sb_{0.33}$ coating Ni 8 nm photoanode.

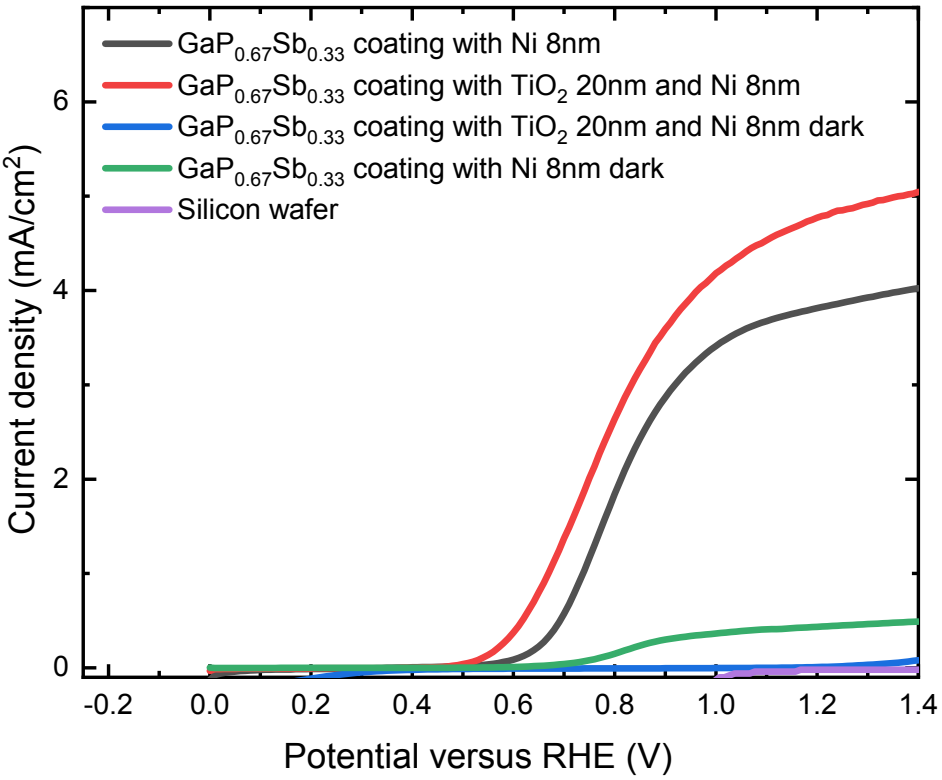


**Figure S6.** Current density versus the potential (*J-V*) curves of $GaP_{0.67}Sb_{0.33}$ photoanodes and Si wafer versus RHE under AM 1.5G simulated 1 sun illumination in 1.0 M KOH electrolyte.

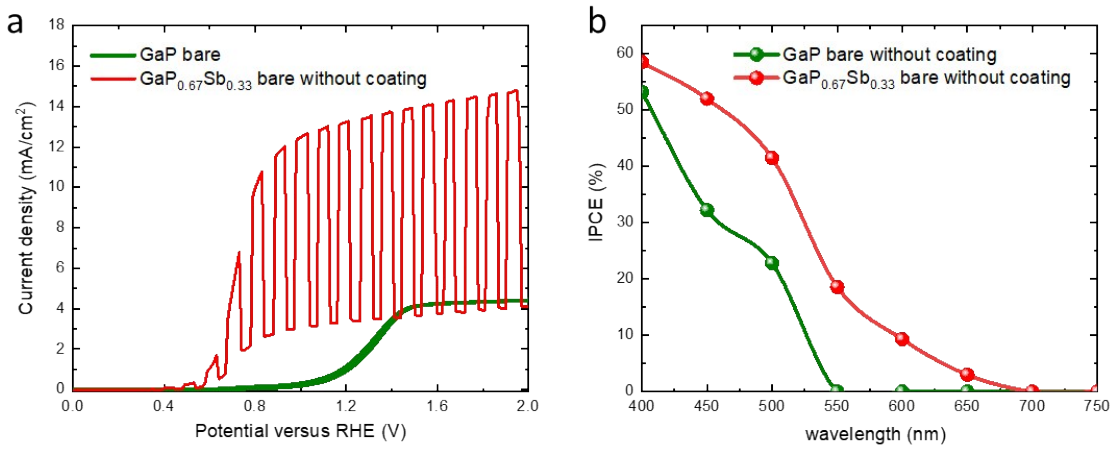


**Figure S7.** (a) Photocurrent density versus potential (*I-V*) curve for GaP and $GaP_{0.67}Sb_{0.33}$ without coating photoanodes under one sun illumination in 1.0 M KOH (pH=14). (b) Spectrum response for GaP and $GaP_{0.67}Sb_{0.33}$ without coating photoanodes in 1.0 M KOH (pH=14) at 1.23 V vs. RHE under the simulated sunlight using an AM1.5G filter.

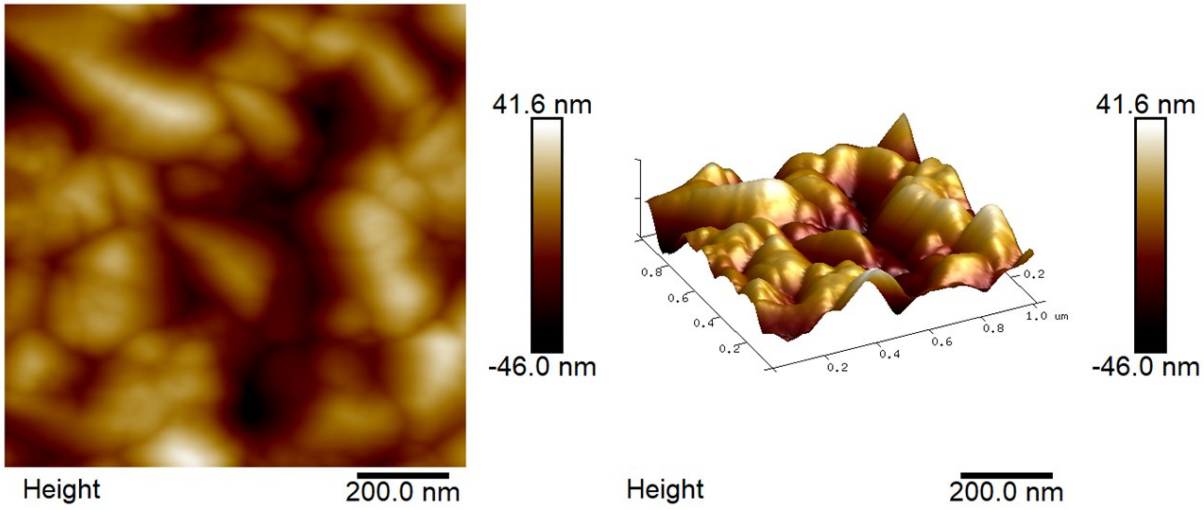


**Figure S8.** Atomic force microscopy image morphology of $GaP_{0.67}Sb_{0.33}$ grown on Silicon substrate as grown by MBE.

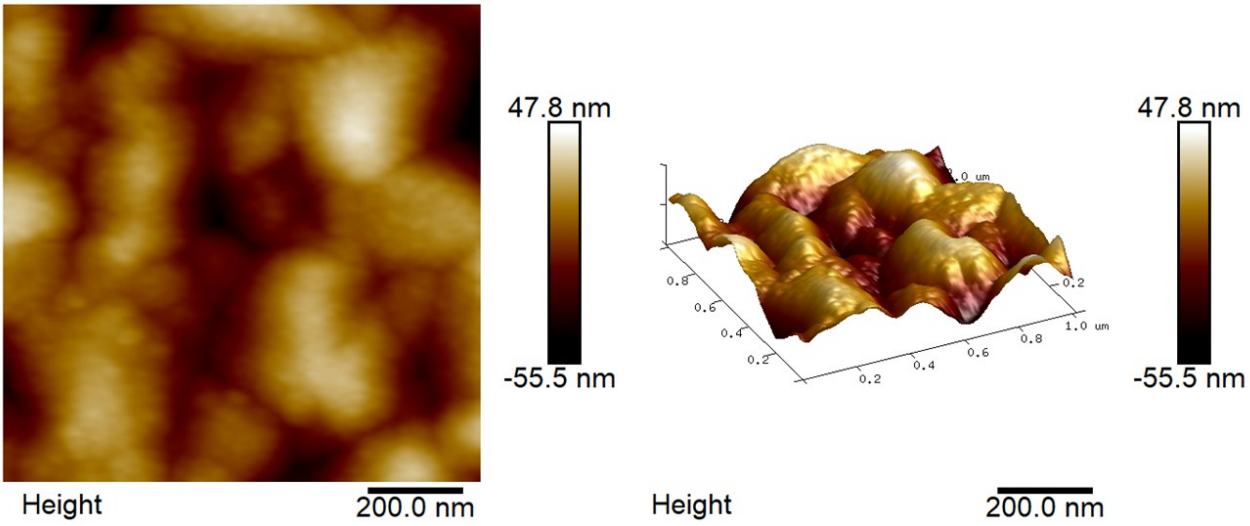


**Figure S9.** Atomic force microscopy image morphology of $GaP_{0.67}Sb_{0.33}$ coating with $TiO_2$ 20 nm and Ni 8 nm photoanode before stability test.

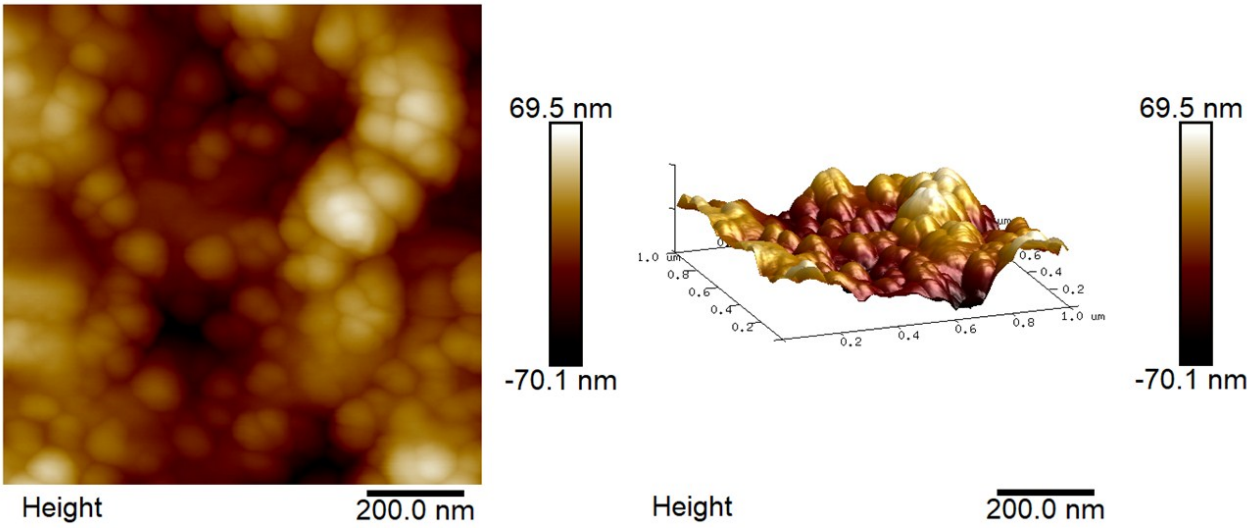


**Figure S10.** Atomic force microscopy image morphology of $GaP_{0.67}Sb_{0.33}$ coating with $TiO_2$ 20 nm and Ni 8 nm photoanode after stability test in 1.0 M KOH (pH=14) solution.

**References:**


1. J. P. Contour, J. Massies and A. Saletes, *Japanese journal of applied physics*, 1985, **24**, L563.
2. S. S. Kher and R. L. Wells, *Chem. Mater.*, 1994, **6**, 2056-2062.
3. R. Nishitani, H. Iwasaki, Y. Mizokawa and S. Nakamura, *Japanese Journal of Applied Physics*, 1978, **17**, 321.
4. F. Garbassi, *Surf. Interface Anal.*, 1980, **2**, 165-169.
5. D. S. Bhachu, R. G. Egdell, G. Sankar, C. J. Carmalt and I. P. Parkin, *Journal of Materials Chemistry C*, 2017, **5**, 9694-9701.
6. N. Kitamura, T. Kikuchi, M. Kakehi and T. Wada, *Japanese Journal of Applied Physics*, 1984, **23**, 1534.
7. W. Yu, J. L. Sullivan and S. O. Saied, *Surf. Sci.*, 1996, **352**, 781-787.
8. T. Nguyen Thanh, C. Robert, W. Guo, A. Létoublon, C. Cornet, G. Elias, A. Ponchet, T. Rohel, N. Bertru, A. Balocchi, O. Durand, J. S. Micha, M. Perrin, S. Loualiche, X. Marie and A. Le Corre, *J Appl Phys*, 2012, **112**, 053521.
9. Y. X. Qiu, M. C. Li, G. J. Liu, B. S. Zhang, Y. Wang and L. C. Zhao, *Journal of Crystal Growth*, 2007, **308**, 325-329.